TOWARDS ACCURATE SPACECRAFT SELF-LOCATION ESTIMATION BY ELIMINATING CLOSE CRATERS IN CAMERA-SHOT IMAGE

Virtual Conference 19–23 October 2020

Yuka Waragai[1], Iko Nakari[1], Yohei Hayamizu[1], Keiki Takadama[1], Hiroyuki Kamata[2]

Takayuki Ishida[3], Seisuke Fukuda[3], Shujiro Sawai[3], Shinichiro Sakai[3]

[1]The University of Electro-Communications, 1-5-1 Chofugaoka, Chofu, Tokyo, 182-8585, Japan
E-mail: {waragai, iko0528, hayamizu}@cas.lab.uec.ac.jp, keiki@inf.uec.ac.jp
[2]Meiji University, 1-1-1 Higashi-Mita, Tama-ku, Kawasaki, Kanagawa, 214-8571, Japan
E-mail: kamata@meiji.ac.jp
[3]Japan Aerospace Exploration Agency, 3-1-1 Yoshinodai, Chuo-ku, Sagamihara, Kanagawa, 252-5210, Japan
E-mail: ishida.takayuki@jaxa.jp, fukuda@isas.jaxa.jp, sawai.shujiro@jaxa.jp, sakai@isas.jaxa.jp

ABSTRACT

This paper focuses on our previous method, Triangle Similarity Matching (TSM), as the conventional method, proposes the method for improving an accuracy of a spacecraft self-location estimation by eliminating the close craters in the camera-shot image, and aims at investigating its effectiveness through the experiment. The proposed method contributes to preventing from wrongly estimating the spacecraft location when two or more craters are close to each other, where the wrong crater may be selected instead of the correct crater. The experiment on the test-case employed in the Smart Lander for Investigating Moon (SLIM) mission have revealed that (1) the estimation accuracy of TSM with the proposed method is better than that of the conventional TSM and (2) TSM with the proposed method was robust to both the images with noise and those with many shadows.

1 INTRODUCTION

In planetary surface exploration, it is important for a spacecraft to land the target exploration area closely as much as possible. To improve the landing accuracy of a spacecraft, the accurate spacecraft self-location estimation method is demanded. For this purpose, Triangle Similarity Matching (TSM) was proposed [1] [2] and improved [3] to estimate the spacecraft self-location by comparing the triangle (composed of three detected craters) in the camera-shot image taken by the spacecraft and the triangle in the crater map (stored in the spacecraft beforehand) as the information on the craters in the planetary surface. TSM can provide the good estimation of the spacecraft location, but its accuracy may decrease when two or more craters are close to each other. This is because the spacecraft self-location can be estimated accurately when the correct crater is selected among the close craters while it is estimated wrongly when the other crater (i.e., the wrong crater) is selected among them. The same problem applies to the line segment matching method described in section 2.1. To overcome this problem, this study proposes the method which improves an accuracy of the spacecraft self-location estimation by eliminating the close craters in the camera-shot image and aims at investigating its effectiveness through the experiment.

This paper is organized as follows. The next section describes TSM, and Section 3 proposes our method for improving an accuracy of a spacecraft self-location estimation. The experiment is conducted and its results are analyzed in Section 4. Finally, our conclusion is given in Section 5.

2 CONVENTIONAL METHOD (TSM)

2.1 Self-Location Estimation by Image-matching Navigation

The self-location estimation method of the spacecraft that we propose is based on the image-matching navigation approach, which takes the following procedures: (1) the spacecraft takes the camera shot image on the planet, and the craters is extracted from the camera shot image, and (2) the self-location of the spacecraft is estimated by comparing the extracted craters with those in the crater database. The detailed procedures are conducted as follows: (1) calculating the crater coordinate as the center position of the crater detected in the camera-shot image taken by the spacecraft; (2) matching the detected crater (precisely, the estimated center of the detected crater) to the crater (precisely, the actual center of the crater) in the crater map stored in the spacecraft, and estimating the self-location of the spacecraft by calculating its coordinate from the crater coordinate in the crater map.

In the case of Smart Lander for Investigating Moon (SLIM) mission which aims at establishing the pin-

point spacecraft landing technology [4], the position of the crater is calculated by Okada et al.'s method [5] for the procedure (1), and the self-location of the spacecraft is calculated by the line segment matching by Kariya et al.'s method [6] or the proposed TSM for the procedure (2). The crater database includes the locations of craters on the moon obtained from Kaguya satellite [7].

2.2 TSM Overview

Figure 1 shows the algorithm flow of TSM. To estimate the self-location of the spacecraft, TSM requires the crater map of the planetary surface (stored in the spacecraft beforehand) and the triangle database (DB) created from the crater map, both of which are stored in the onboard computer of the spacecraft. Since matching with all the craters takes a long time, as shown in the lower part of Figure 1, TSM constructs a triangle DB consisting of three craters that satisfy a certain condition from all the craters, and matches the triangles to each other to save time. As shown in the upper part of Figure 1, the TSM estimates the self-location of the spacecraft based on the crater map and the crater triangle DB as follows:

(1) Create a triangle consisting of three craters from the craters detected in the camera-shot image;

(2) Compare the triangles in the camera-shot image with those in the crater triangle DB;

(3) After TSM detects the triangle in the camera-shot image which is matched with that in the triangle DB, TSM checks whether the craters around the triangle in the camera-shot image match with the those in the crater map (note that the matched craters are called as the pairing craters in this paper);

(4) If the number of pairings is less than a certain threshold, then return to (2), and if not, TSM estimates the current self-location of the spacecraft by the matched triangular craters and the pairing craters.

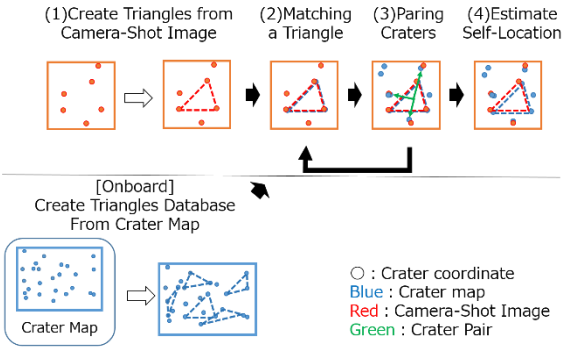

Figure 1: Algorithm flow of TSM

2.3 The Crater Triangles DB

The crater triangles DB contains the three crater coordinates of the three points, the angles of the three corners, and the lengths of the three sides of created triangles in ascending order, and the Area Number of the center of gravity of the triangles. This Area is a section of the crater map divided into 240 plots of non-overlapping length and width, which can reduce the computational cost of the matching process.

2.4 Triangle Matching

TSM determines whether the triangle in crater triangles DB and that in the camera-shot image are matched or not by the difference of ratio of the lengths of the sides and the difference of the angular between them. Concretely, the two triangles are determined to be matched if the ratio of the three sides is greater than 0.8 and less than 1.2, respectively, and if the difference between the three angles is less than the certain threshold value. Equation (1) shows the conditional expression for the angle, where the i is numbered from the largest angle, and θ_i and θ_i' are the angles of the crater triangles DB and the triangles in the captured image respectively. Equation (1) takes the cosine of the angle of the triangle and sums the absolute values of the differences and compares them to the threshold mindiff.

$$\sum_{i=1}^{3} |cos\theta_i' - cos\theta_i| < \text{mindiff} \qquad (1)$$

2.5 Craters Pairing

After matching that the triangle in the crater triangles DB and the triangle in the camera-shot image are matched, TSM determines whether the craters around each triangle are identical or not. Figure 2, consisting of two diagrams, shows an example of crater pairing. The diagram on the left shows the crater map, and the diagram on the right shows the camera-shot image, where the yellow dots indicate the centers of gravity of each triangle and the light blue and orange dotted lines indicate the matching triangles. The dark blue and red lines indicate the vector of the long side of the triangle $\overrightarrow{d_l}$, $\overrightarrow{d_l'}$ and the vector extending from the center of gravity to the craters around the triangle $\overrightarrow{d_c}$, $\overrightarrow{d_c'}$. TSM determines if the craters around the triangle in the crater map and those in the camera-shot image are identical craters based on the inner and outer products of these two vectors. Concretely, the ratio of the length of the long sides is calculated by Equation (2), and the inner and outer product differences are calculated by Equations (3) and (4). Then, if the inner product difference I < threshold TH1, and the outer product difference C < threshold TH2, and the sum of I and C < threshold TH3, the craters around the triangles in the

crater map and those in the camera-shot image are determined to be identical craters (i.e., pairing is possible) in Equation (5). Figure 3 shows the acceptable range according to the Equation (5), where the vertical axis indicates the value of C and the horizontal axis indicates the values of I. The acceptable range is inside the green line as shown in the Figure 3. Note that TH1 and TH2 are set to the same value.

$$\gamma = \frac{\left|\overrightarrow{d_l'}\right|}{\left|\overrightarrow{d_l}\right|} \tag{2}$$

$$I = \left|\overrightarrow{d_l} \cdot \overrightarrow{d_c} - \frac{\overrightarrow{d_l'} \cdot \overrightarrow{d_c'}}{\gamma^2}\right| \tag{3}$$

$$C = \left|\overrightarrow{d_l} \times \overrightarrow{d_c} - \frac{\overrightarrow{d_l'} \times \overrightarrow{d_c'}}{\gamma^2}\right| \tag{4}$$

$$(I < TH1) \wedge (C < TH2) \wedge (I + C < TH3) \tag{5}$$

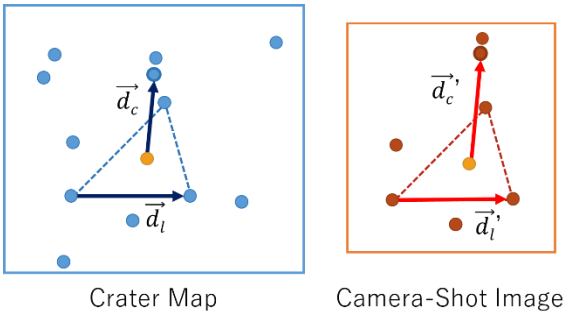

Figure 2: Craters Pairing

Furthermore, to prevent the accumulation of misalignments in the same direction, TSM calculates the sum of the total of the outer product differences and that of the inner product differences for all the craters around the triangle determined to be identical craters. If the absolute value of the sum of either or both of the inner and outer product differences is greater than or equal to the threshold value, the crater which has the equal sign with calculated total of the inner and outer product differences and largest value among the group of craters is removed from the pairing craters.

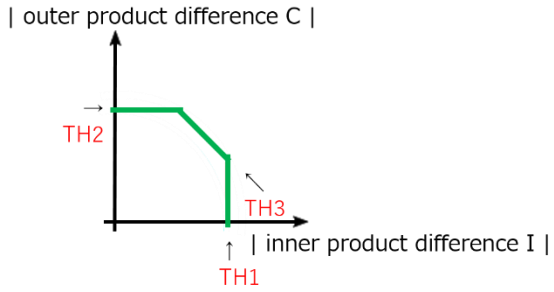

Figure 3: Range of Paring Craters

2.6 Algorism

In TSM, as shown in Figure 4, the method of self-location estimation is changed according to the number of pairing craters. The specific methods, depending on the number of paring craters, are as follows:

(1) If the difference between inner and outer product difference shown in Figure 3 is within the thresholds TH1' (< TH1) and TH2' (< TH2) respectively, and if the number of paring craters, which has the sum of the inner and outer product differences is within the threshold TH3' (< TH3), is X (> Y) or more, the method calculates the self-location coordinates by the coordinates of the craters which are forming the triangle and the paring craters around the triangle;

(2) If the number of pairing crater, which has the inner and outer product differences within the threshold value TH1 (=TH2) as shown in Figure 3, is greater than or equal to Y, the method calculates the self-location coordinates by the coordinates of the craters which are forming the triangle and the pairing craters around the triangle;

(3) If the number of pairing craters, which has the inner and outer product differences within the threshold TH1 (= TH2) as shown in Figure 3, is less than Y, the method archives the paring craters and the craters which are forming the triangle. Then, return to (1) to get another triangle match (but not if the number of pairing craters saved so far is large);

(4) If the maximum number of pairing craters, which is archived through matching with all the triangles in the crater triangles DB, is less than Z, the method determines the estimation failure because the accuracy of the self-location estimation cannot guaranteed.

Note that, X, Y and Z are hyper parameters.

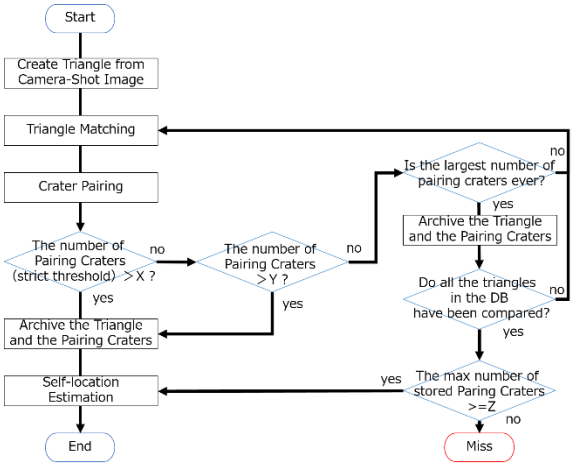

Figure 4: Algorism

3 PROPOSAL METHOD

In the conventional TSM, accuracy of self-location estimation may decrease when the craters are dense. To overcome that issue, the proposed method, shown in Figure 5, removes the proximate craters from the matching target by introducing the method between (2) and (3) in Figure 1, which shows the processing of the TSM. In Figure 5, blue colors show the crater map, orange colors show the camera-shot image, the dots indicate the detected craters, and the dotted lines indicate the matched triangles. The algorithm of the proposed method is as follows:

(1) TSM matches the triangle in the camera-shot image with that in the crater triangles DB;
(2) Calculate the total distance D (the sum of the distances indicated by the green line in Figure 5 (2)) of all crater combinations in the camera-shot image;
(3) As indicated by the green cross mark in Figure 5 (3), the proposed method removes the craters of the camera-shot image when the distance between the craters is less than or equal to the threshold TH calculated by the equation (6). where the N indicates the total number of craters and the a indicates the coefficient.

$$\mathrm{TH} = \frac{D}{{}_N\mathrm{C}_2} * a \qquad (6)$$

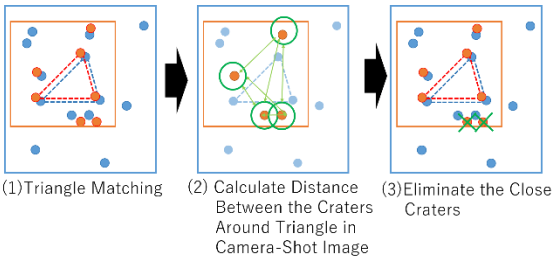

Figure 5: Calculate Distance and Elimination

The important point in the proposed method is that since it is not possible to determine which of the proximity craters is correct, both proximity craters should be removed.

However, the more the craters are removed, the lower the accuracy of self-location estimation is likely to be, the proposed method is not applied in the following cases.

- A case in which the number of paring craters becomes less than Y by removing the craters in the camera-shot image and TSM have to start matching with another triangle.
- A case in which the number of pairing craters is reduced from more than X to less than X by removing craters in the camera-shot image.
- A case in which the number of pairing craters is reduced from more than Y to less than Y by removing craters in the camera-shot image.

4 EXPERIMENT

4.1 Experimental Settings

In order to verify the effectiveness of the proposed method, TSM with the proposed method is compared with a conventional TSM on a test set employed in a SLIM mission. The test set consists of four patterns based on the lunar crater map and the presumed image (Pattern types are shown in Table 1). These patterns assume both nominal and back-up trajectories with and without noise. The noise includes differences in brightness and contrast, distortion, bokeh, peripheral attenuation, brightness fluctuation, slight shifting, and radiation noise. The back-up orbit has a different solar altitude than the nominal case and has many shadows in the image. Each test pattern contains 1000 images.

Table 1: Classification of Test Patterns

	Nominal	Back-up Orbit
No Noise	6710	6760
Noised	6810	6860

4.2 Evaluation Criteria and Parameter

The estimation accuracy is used as the evaluation criterion and is compared by estimation category and estimation error. The estimation categories are classified as “Great”, “Good”, and “Misjudgment” when the distance between the estimated coordinate of the spacecraft and the correct coordinate is less than or equal to 3 pixels, less than or equal to 7 pixels, and farther than 7 pixels in both x and y coordinates respectively. When the spacecraft fails to estimate its own coordinate for a case, the case is labeled as “Miss Matching”. A large amount of “Great” label indicates high estimation accuracy. Estimation error evaluates the mean, and maximum values of the estimation result in all the cases, allowing detailed analysis.

The values shown in Table 2 are used as parameters. TH1, TH2, TH3, TH1’, TH2’, and TH3’ have different values because the length of the triangle’s long side $|\overrightarrow{d'_l}|$ triangle in the camera-shot image varies in different cases.

Table 2: parameter value

Parameter Name	Value	Notes
mindiff	93	
TH1	150 * $|\overrightarrow{d'_l}|$	TH1=TH2
TH2	150 * $|\overrightarrow{d'_l}|$	TH2=TH1
TH3	220 * $|\overrightarrow{d'_l}|$	
TH1’	100 * $|\overrightarrow{d'_l}|$	Strict threshold
TH2’	100 * $|\overrightarrow{d'_l}|$	Strict threshold
TH3’	50 * $|\overrightarrow{d'_l}|$	Strict threshold
X	14	Judging the number of craters paired using strict thresholds
Y	9	Judging the number of all pairing craters
Z	5	Minimum number of pairing craters to determine self-location estimation
a	1/8	Equation (6)

4.3 Result

Table 3 shows the experimental results: rows 1-2 show the types of test patterns, rows 3-6 show the estimation categories and their number of cases, rows 7-8 show the mean and maximum values of estimation error, columns 3-6 show the results of conventional TSM and columns 7-10 show the results of TSM with the proposed method. The cells is colored green, red, and white, in which TSM with the proposed method is better, worse, no change compared to the conventional method. Table 3 shows that there is no change in the number of cases and the maximum estimation error in the estimation categories, but the mean value of the estimation error improves for the three test patterns 6710, 6760 and 6860.

Figure 6 and Figure 7 are reported for detailed analysis which cases affect to the result of Figure 3. Figure 6 shows the number of cases where the estimation accuracy is improved or deteriorated. The vertical axis in Figure 6 indicates the number of cases that improved or deteriorated, and the horizontal axis indicates the type of test pattern. Figure 7 shows the degree of improvement or deterioration of the estimation accuracy (the average of differences of “improved or worsened estimation errors” from the conventional method). The vertical axis in Figure 7 represents the degree of improvement or deterioration (in pixels) and the horizontal axis represents the type of test pattern.

In both figures, blue indicates improvement and orange indicates deterioration.

Table 3: Result

test patterns		conventional method				proposal method			
		6710	6760	6810	6860	6710	6760	6810	6860
Estimation Result [the number of case]	Great	1000	1000	998	999	1000	1000	998	999
	Good	0	0	2	1	0	0	2	1
	Misjudgment	0	0	0	0	0	0	0	0
	Miss Matching	0	0	0	0	0	0	0	0
Estimation Error Value [px]	Average	1.052	1.252	1.079	1.275	1.0476	1.2241	1.081	1.2452
	Maximum	3.061	3.262	3.762	3.535	3.061	3.262	3.762	3.535

Figure 6 and Figure 7 show that the test pattern 6710 has a large number of improvements, while the degree of improvement and the degree of deterioration are about the same. 6760 has a high degree of improvement and a large number of improvements. The number of improved cases and the number of cases worsened were about the same for 6810, but the degree of deterioration was high. 6860 has the same trend as 6760. These results show that the proposed method is valid, except 6810.

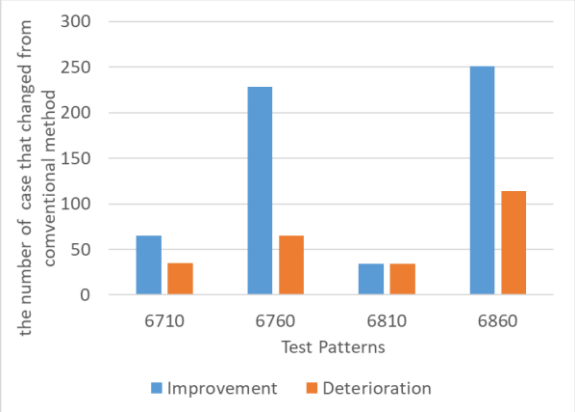

Figure 6: Number of cases in which the accuracy of self-location estimation improved or deteriorated

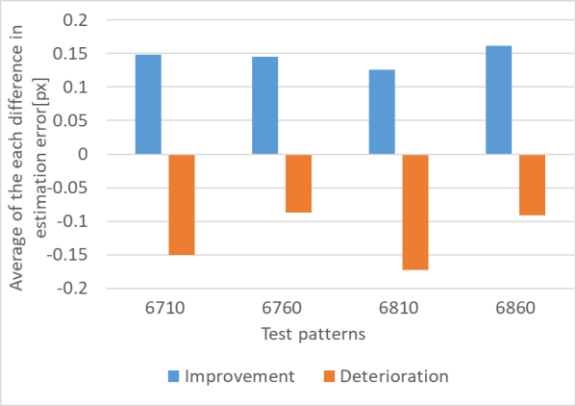

Figure 7: the degree of improvement or worsening of the accuracy of self-location estimation (the average of "estimation errors of conventional method minus improved or worsened estimation errors")

4.4 Discussion

- Deletion of the close craters

The proposed method removes close proximity craters from the camera-shot image to improve the estimation accuracy. Picking up a case, we analyze how the proposed method works on self-location estimation. The visual images of the coordinates of craters selected for pairing and the triangles matched with the triangular database are shown in Figure 8. In this analysis, the case number52 in 6760 is selected because this case turned from “Good” to “Great” through the experiment. Camera-shot images are represented in red and crater maps in blue. Triangles composed of three lines represent paired triangles. Circles represent the coordinates of the detected craters. Crosses represent the coordinates of pairing craters. The pairs of blue and red “Circle and Cross” with the same number in the upper right corner are selected craters for pairing. The green arrows indicate the craters selected in the conventional method but removed in the proposed method.

In Figure 8 and Figure 9, (a) shows the results of the conventional method, and (b) shows the results of the proposed method.

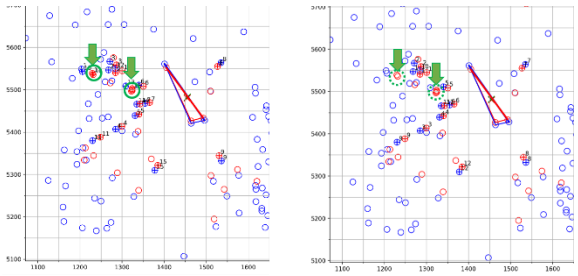

Figure 8: Changes in the case number52 in 6760

From Figure 8, it can be seen that in (b), pairing craters 1, 10 and 13 are removed compared to (a). In particular, in (a) No. 13, the craters detected in the camera-shot image are in close proximity to each other, and the craters are removed, and the proposed method accurately removes the close craters. This result shows that removing appropriate craters from the camera-shot image improves the estimation accuracy.

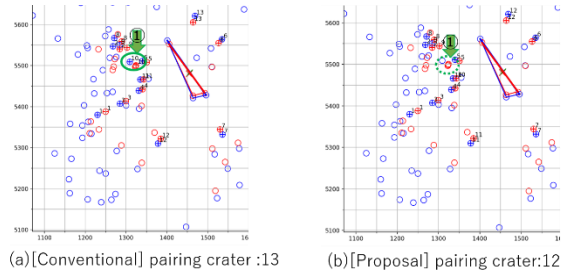

Figure 9: Changes in the case number52 in 6860

From Figure 9, it can be seen that in (b), pairing crater No.10 is removed compared to (a). In (a) No.10, the crater detected in the camera-shot image is also in close proximity to each other. Since Figure 9 shows a shadowed test pattern, the number of craters detected is smaller than that in Figure 8. So, if the wrong pairing craters are used for self-location estimation, the accuracy is worse than if the number of craters around the triangle is large. However, the accuracy of self-location estimation can be improved by precisely removing the craters detected in close proximity.

- An effectiveness of proposal method against shadowy hours

The four test patterns used in this paper are generated from two different trajectories. Using these different patterns for validation provides insights into the impact arising from sources other than noise. As noted in the “Result” section, Figure 6 shows that the number

of improvements case in test patterns 6760 and 6860 is higher than in 6710 and 6810. Considering that both 6760 and 6860 are images of back-up orbits, and the low solar altitude causes shadows, there is a high possibility that the center coordinates of the craters can be displaced, and craters that are not close to each other can be placed close to each other. It can be said that the proposed method succeeds in removing them from the objects of self-location estimation. Furthermore, Figure 7 shows a greater degree of improvement than the degree of deterioration in the test patterns 6760 and 6860, as well as the improvement with regard to the number of "Great" cases. This result also shows that the proposed method is successful for the effect of shadows caused by low solar altitude, i.e., the proposed method is more useful during shadowy hours. On the contrary, 6710 and 6810 show less displacement of the crater center coordinates (fewer craters placed in close proximity by mistake). Therefore, there is no difference between improvement and deterioration in 6710 and a higher degree of deterioration in 6810. This deterioration is caused by the removal of the correct craters that are in close proximity to the original.

Figure 10 shows the matched triangles' coordinates and pairing craters in The case number52 for test patterns 6710 (few shadows) and 6760 (many shadows) to validate the above analysis. The results for 6710 and 6760 are shown in (a) and (b) of the figures. Note that the horizontal and vertical axes, lines, red and blue circles, "Circles and Crosses", and the numbers in the upper right corner of "Circles and Crosses" in the figure have the same meaning as explained in Figure 8. The number (1) on the green allow in Figure 10 shows the double detection by the shadow. The number (2) on the green allow in Figure 10 is not present in (a), but it is closely detected in (b). This figure shows that the craters detected in back-up orbit caused by shadowing but not detected in the nominal state, are close to each other, and the proposed method can remove these close craters.

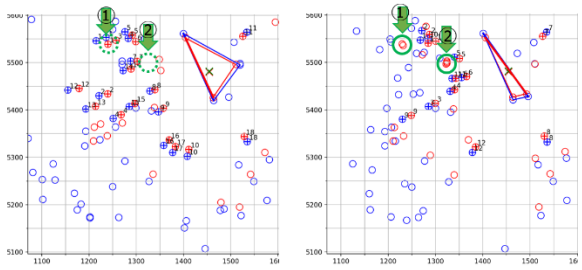

(a) Test pattern 6710 (b) Test pattern 6760

Case No.52

Central coordinate of this image(1454.6, 5480.4)

Figure 10: Comparison of the 6710 and the 6760

- A Robustness of Proposal Method for Noise

Figure 6 shows no significant difference in the number of cases with or without noise (test patterns 6710 and 6810, and test patterns 6760 and 6860) that were improved or worsened. This fact shows that the proposed method is robust to noise. To validate the above analysis, Figure 11 and Figure 12 show the matching triangles' coordinates and pairing craters' coordinates for The case number52 for 6710 (no noise) and 6810 (no noise) and The case number52 for 6760 (no noise) and 6860 (noise). In both figures, (a) shows the 6710/6760 results and (b) shows the 6810/6860 results. Note that the horizontal and vertical axes, lines, red and blue circles, "Circles and Crosses", and the numbers in the upper right corner of "Circles and Crosses" in the figure have the same meaning as in Figure 8.

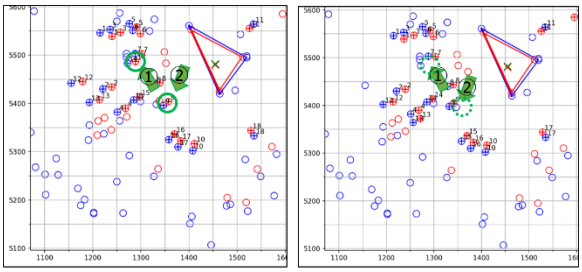

(a) Test pattern 6710 (b) Test pattern 6810

Case No.52

Central coordinate of this image (1454.6, 5480.4)

Figure 11: Comparison of the 6710 and the 6810

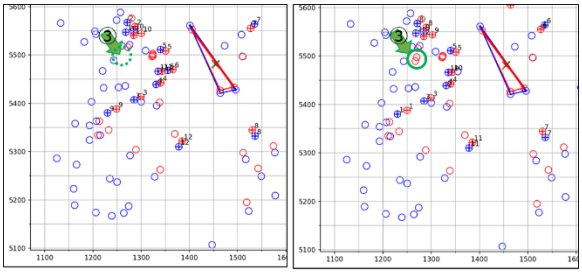

(a) Test pattern 6760 (b) Test pattern 6860

Case No.52

Central coordinate of this image (1454.6, 5480.4)

Figure 12: Comparison of the 6760 and the 6860

From these figures, a comparison of the craters detected around the center coordinate of the images of 6710 and 6810 (1454.6, 5480.4) shows that new craters are detected or not detected after the addition of noise (numbers (1) and (2) in Figure 11). Similarly, for the back-up orbits 6760 (no noise) and 6860 (with noise), new craters are detected or not detected after the addition of noise (see Figure 12, (3)). Regardless of the presence or absence of such detected craters, the proposed method finds the pairing of the craters

around the triangle and contributes to the situation of the accuracy of self-location estimation.

5 CONCLUSION

This study proposed the method for TSM to improve an accuracy of a spacecraft self-location estimation by eliminating the close craters in the camera-shot image. The proposed method successfully reduced the number of cases where the wrong craters are selected. Compared to the conventional TSM, the following implications have been revealed: (1) the accuracy of a spacecraft self-location of TSM with the proposed method is better than that of TSM, and (2) TSM with the proposed method was robust to both the images with noise and those with many shadows.

The following research must be done in near the future: (1) an investigation of robustness of the proposed method in other situations, and (2) an improvement of the methods to find the "Great" location from the "Good" location found by TSM.

References

[1] Ishii, H., Umenai, Y., Matsumoto, K., Uwano, F., Tatsumi, T., Takadama, K., Kamata, H., Ishida, T., Fukuda, S., Sawai, S., Sakai, S., "How to Detect Essential Craters in Camera Shot Image for Increasing the Number of Spacecraft Location Candidates while Improving Its Estimation Accuracy?", *The 14th International Symposium on Artificial Intelligence, Robotics and Automation in Space (i-SAIRAS2018)* (2018).

[2] Ishii, H., Murata A., Uwano F., Tatsumi T., Umenai, Y., Takadama, K., Harada T., Kamata, H., Ishida T., Fukuda S., Sawai S., Sakai S., "Improvement of the SLIM spacecraft location estimation by crater matching based on similar triangles and its improvement", *Aerospace technology*, Vol. 17(2018), pp. 69 – 78 (in Japanese).

[3] Waragai, Y., Uwano, F., Takadama, K., Kamata, H., Ishida, T., Fukuda, S., Sawai, S., Sakai, S., "Improvement estimation of Self-Positioning Accuracy of SLIM Spacecraft Using Coordinate Shift of Crater", *Proceedings of the Space Sciences and Technology Conference*, 64, JSASS-2019-4019 (2019) (In Japanese).

[4] JAXA/ISAS, "A proposal of Smart Lander for Inv estigating Moon", Available at https://global.jaxa.jp/projects/sas/slim/

[5] Okada, S., Nakahama, Y., Moribe, M., Kamata, H., Kariya, K., Takadama, K., Ishida, T., Fukuda, S., Sawai, S., Sakai, S., "Detection of the Position and the Size of Craters using Principal Component Analysis and its Evaluations", *Aerospace technology*, Vol. 17 (2018) pp. 61-67 (in Japanese).

[6] Kariya, K., Ishida, T., Sawai, S., Kinoshita, T., Kajihara, K., Iwasa, O., Fukuda, S., "Position Estimation Using Crater-based Linear Features for Pinpoint Lunar Landing", *Aerospace technology*, Vol.17 (2018) pp. 79-87, 2018 (in Japanese).

[7] Kaku, T., Haruyama, J., Miyake, W., Kumamoto, A., Ishiyama, K., Nishibori, T., Howell, K.C.: "Detection of intact lava tubes at Marius Hills on the Moon by SELENE (Kaguya) lunar radar sounder", *Geophysical Research Letters*, Vol. 44, pp. 10,155-10,161, 2017.